Journal of Power Sources 195 (2010) 3140–3144

Contents lists available at ScienceDirect

Journal of Power Sources

journal homepage: www.elsevier.com/locate/jpowsour

Short communication

Regenerating Pt–3d–Pt model electrocatalysts through oxidation–reduction cycles monitored at atmospheric pressure

Carl A. Menning, Jingguang G. Chen*

Department of Chemical Engineering, Center for Catalytic Science and Technology, University of Delaware, 150 Academy St., Newark, DE 19716, United States

ARTICLE INFO

Article history:
Received 15 October 2009
Received in revised form
22 November 2009
Accepted 25 November 2009
Available online 2 December 2009

Keywords:
Oxygen
Hydrogen
Segregation
Nickel
Platinum

ABSTRACT

The interchange between the Pt–Ni–Pt and Ni–Pt–Pt bimetallic configurations in O_2 and H_2 is confirmed experimentally at atmospheric pressure using in situ X-ray absorption spectroscopy (XAS). The subsurface Pt–3d–Pt structure, a desirable configuration as cathode electrocatalysts for PEM fuel cells, is found to be preferred in the reducing environment of H_2 whereas the surface 3d–Pt–Pt configuration is preferred in O_2. This process has been found to be reversible, providing useful insights into the maintenance and regeneration of the desirable subsurface structure.

1. Introduction

The subsurface Pt–3d–Pt structures, where 3d represents Ni, Co, Fe, Mn, Cr, V, and Ti, have been identified as promising catalysts for a wide range of applications, from the oxygen reduction reaction (ORR) at the cathode of PEM fuel cells [1] to hydrogenation reactions in heterogeneous catalysis [2,3]. These bimetallic surfaces have been shown to span a wide range of chemical and physical properties beyond a simple combination of the parent metal properties [4–6]. The unique properties of the subsurface Pt–3d–Pt bimetallic structures are due to the strain effect from lattice mismatch between alloy metals and the electronic effect related to the difference in electronic configuration [7]. However, one of the challenges in the application of these bimetallic structures is the tendency of the subsurface 3d atoms to segregate on top of the surface Pt layer, therefore losing the desirable electrocatalytic and catalytic properties. The ability to maintain and/or regenerate the desirable Pt–3d–Pt subsurface structure is of critical importance for their applications in fuel cells and hydrogenation reactions.

Several recent fundamental surface science and theoretical studies have been performed to determine the thermodynamic stability and kinetic transformation of the Pt–3d–Pt subsurface structures [4]. The surface science experiments have been typically performed under ultra-high vacuum (UHV) conditions detailing the stability under a number of reaction environments, such as in low pressure of hydrogen and oxygen. However, the extension of these UHV studies to atmospheric conditions, which are more relevant to the maintenance and regeneration of the subsurface structures, has yet to be established. This is mainly due to the difficulty in the in situ measurements of spectroscopic changes from the interchange between the surface and subsurface structures at higher pressures. The current communication will detail a novel approach to quantify metal segregation at atmospheric pressure by monitoring monolayer bimetallic surfaces prepared in UHV and subsequently exposed to hydrogen and oxygen at atmospheric conditions. The changes in the surface composition, from the diffusion and segregation of the 3d metals, were monitored using the white line of the 3d metals with X-ray absorption spectroscopy (XAS). Due to the high intensity and energy of the synchrotron radiation, XAS offers the unique advantage to monitor changes in monolayer coverages under in situ reaction conditions.

In addition to determining the activation barriers for the diffusion and segregation of 3d metals in Pt–3d–Pt, the current study is also focused on bridging the pressure gap from UHV to atmospheric pressure to more closely resemble the conditions in heterogeneous catalysis and electrocatalysis. Previous studies by this group have aimed at bridging the materials gap of Pt–3d–Pt bimetallic structures prepared on single crystal Pt(1 1 1) [8] and on polycrystalline Pt foils [9] to incorporate both the additional (1 0 0) crystal facet as well as lower coordinated sites found on supported nanoparticles. Qualitatively, both single crystal and polycrystalline bimetallic systems displayed similar behaviour in the environments probed.

* Corresponding author. Tel.: +1 302 831 0642; fax: +1 302 831 2085.
E-mail address: jgchen@udel.edu (J.G. Chen).

0378-7753/$ – see front matter © 2009 Elsevier B.V. All rights reserved.
doi:10.1016/j.jpowsour.2009.11.109

The subsurface Pt–3d–Pt structure was thermodynamically preferred in vacuum and the subsurface 3d metals were drawn to the surface using oxygen to form the surface 3d–Pt–Pt configuration [8,9]. Using these fundamental understandings from UHV measurements, the current study is focused on bridging the pressure gap and demonstrating that similar segregation kinetics is present at more applicable pressures.

2. Methods

2.1. Techniques

The samples were prepared in a UHV system and characterized using X-ray photoelectron spectroscopy (XPS) in a chamber with a base pressure of 4×10^{-9} Torr, as described previously [9]. Ni and Co were deposited using line-of-sight physical vapor deposition (PVD). X-ray absorption spectroscopy (XAS) was performed on beamline X-18b at the National Synchrotron Light Source (NSLS) at Brookhaven National Laboratory. The samples were exposed to 5% H_2 in He or 10% O_2 in He using an in situ reaction cell. The temperature was monitored using a K-type thermocouple.

2.2. Sample preparation

The Pt foil sample was cut from a larger polycrystalline Pt foil (99.95%) with a thickness of 0.004 mm. The foil was affixed onto two tantalum posts by crimping a Ta frame around the edge of the foil to maintain physical contact. The posts were used as electrical and thermal contacts for resistive heating, which allowed the temperature of the Pt foil to be varied between 300 K and 1200 K. The temperature was monitored by a K-type thermocouple welded to the back of the foil. The surface was cleaned by successive cycles of sputtering Ar^+ followed by annealing in vacuum to 1050 K until the surface contaminants, such as C and O, were below the detection limit of XPS.

The Ni/Pt or Co/Pt bimetallic surfaces were prepared by evaporating Ni or Co by line-of-sight physical vapor deposition (PVD) onto the Pt foil using a high-purity Ni (99.994%) or Co (99.999%) wire wrapped around a tungsten filament. The Pt foil sample was at a temperature of 300 K during deposition. The coverage of the Ni or Co overlayer was estimated using the Ni($2p_{3/2}$)/Pt(4f) or Co($2p_{3/2}$)/Pt(4f) XPS ratio as described in our previous studies on the Co/Pt(1 1 1) surface [10] or estimated by screening calculations using inelastic mean free paths (IMFP) from [11].

3. DFT predicted segregation energy of Pt–3d–Pt(1 1 1) in vacuum, H_2, and O_2

3.1. Method

The *ab initio* calculations were performed using the Vienna *Ab initio* Simulation Package (VASP) version 4.6 [12–14]. The monolayer bimetallic systems were modeled using the closed-packed fcc(1 1 1) surface of the host metal, Pt. The PW91 functional was used within the generalized gradient approximation with an energy cutoff on the basis set of 396 eV. The bimetallic systems were modeled using a periodic 2×2 unit cell with four metal layers. The slabs were separated by 6 equivalent layers of vacuum in the epitaxial direction. The surface 3d–Pt–Pt(1 1 1) configuration was modeled with the first layer composed of the admetal and the remaining three layers composed of Pt. The subsurface Pt–3d–Pt(1 1 1) configuration had the Pt metal in the first, third, and fourth layers while the second layer was completely substituted with the admetal. The top two layers were allowed to relax to the lowest energy configuration while the third and fourth layers were frozen at the bulk host metal distance of 2.83 Å for Pt, as previously determined for the PW91 exchange/correlation functional [15]. A Monkhorst–Pack k-point mesh of $3 \times 3 \times 1$ was used, having 5 irreducible k-points in the first Brillouin zone. This has been shown to be sufficient for the current study as previous studies have shown negligible change in the results for higher k-point meshes [16]. For the convergence criteria of the energy minimization, the calculations were iterated until the total energy change between ionic steps was less than 0.0001 eV. The d-band center of mass was calculated by projecting the plane waves onto spherical harmonic orbitals. The d-band center of mass for this paper is defined as the first moment of only the d-orbital bands that have some degree of electron occupation for the four surface atoms using a Gaussian smearing method between k-points and a short cut-off radius of 1.5 Å. The segregation energy in hydrogen and oxygen was simulated using a coverage of 0.5 ML. This coverage was modeled by placing two separate H or O atoms in 3-fold hollow sites per unit cell.

3.2. DFT predictions

The thermodynamically preferred configuration is directly related to the chemical environment present on the surface. Fig. 1 shows the predicted potential for segregation for a 3d metal atom to go from the subsurface to the surface and the value is scaled per Pt–3d metal pair. These values were calculated for the environments of vacuum, and with 0.5 monolayer (ML) atomic hydrogen and 0.5 ML atomic oxygen, using procedures described previously [16]. The thermodynamic potential for segregation is defined as follows:

$$\Delta E_{seg} = \frac{E_{A/3d-Pt-Pt} - E_{A/Pt-3d-Pt}}{M} \quad (1)$$

where ΔE_{seg} is the thermodynamic potential for segregation per Pt–3d pair, $E_{A/3d-Pt-Pt}$ is the total energy for the surface configuration with adsorbate A, $E_{A/Pt-3d-Pt}$ is the total energy for the subsurface configuration with adsorbate A, and M is the total number of Pt–3d pairs per unit cell.

As defined in a previous publication [17], a positive ΔE_{seg} value indicates that the subsurface Pt–3d–Pt is more stable. The DFT results in Fig. 1 predict that for the reducing environment of vacuum and 0.5 ML atomic hydrogen, the subsurface configuration is

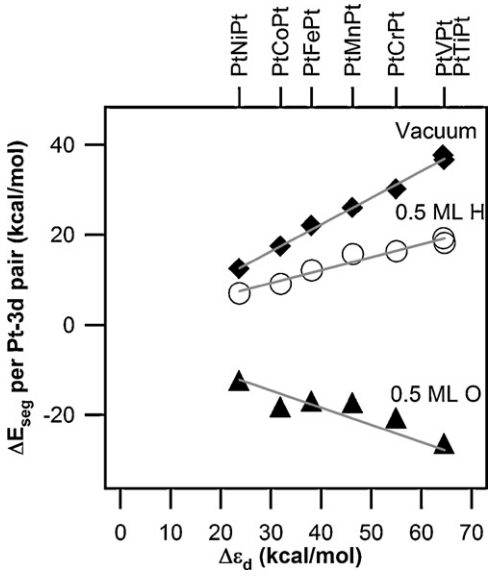

Fig. 1. Correlation between thermodynamic potential for segregation, ΔE_{seg} and the difference in d-band center, $\Delta \varepsilon_d$, for Pt–3d systems exposed to vacuum, and with 0.5 ML atomic hydrogen and 0.5 ML atomic oxygen.

thermodynamically preferred whereas in 0.5 ML atomic oxygen, the surface configuration is preferred. There is a nearly linear trend with the difference in d-band, $\Delta\varepsilon_d$, with Pt–Ni–Pt(1 1 1) having the smallest potential and Pt–Ti–Pt(1 1 1) the largest for diffusion/segregation of the 3d atoms.

4. Experimental results

As demonstrated previously, Ni or Co can be deposited on the Pt substrate layer-by-layer in UHV at room temperature, leading to the formation of the surface 3d–Pt–Pt configuration [3]. Alternatively, if the surface is annealed in vacuum to 600–700 K, the 3d metal can be driven inwards to create the subsurface Pt–3d–Pt configuration [3]. The same procedure was used for preparing the surface and subsurface structures in the current study, except on ultra-thin polycrystalline Pt foil (~4 μm thick) to reduce the self-absorption in XAS measurements. Briefly, monolayer Ni or Co was deposited using line-of-sight physical vapor deposition in UHV. Fig. 2 shows the characteristic Ni K edge spectra for the as-prepared PtNiPt and NiPtPt foil samples prepared in UHV. The surface NiPtPt sample has a higher white line peak intensity at 8351 eV compared to the subsurface PtNiPt sample, which is attributed to the removal of valence electrons from Ni due to oxidation of the surface Ni atoms [18]. There is an additional Ni K-edge feature for the PtNiPt sample at 8374 eV, which is not present for the NiPtPt sample. This peak is in the spectroscopic region assigned to multiple scattering events from more delocalized states. Due to these complex scattering events, features in this region are more sensitive to the changes in the neighbouring shells of atoms surrounding the element of interest [18–20]. The 8374 eV feature may capture the configuration interchange since Ni atoms in the subsurface structure have a complete first shell and more complete higher order shells whereas those in the surface structure do not.

The comparison in Fig. 2 qualitatively confirms that XAS can capture the difference between surface NiPtPt and subsurface PtNiPt in the as-prepared samples. These characteristic spectroscopic features are then used to determine the diffusion and segregation kinetics of Ni atoms. The bottom set of spectra in Fig. 3a shows the comparison of an initially UHV prepared NiPtPt sample before and after multiple cycles of oxidation in O_2 and reduction in H_2 at 693 K. The changes between the two spectra in Fig. 3a mimic the differences seen between the as-prepared PtNiPt and NiPtPt scans in Fig. 2, indicating that the interchange between the surface and subsurface structures can occur from oxidation and reduction cycles. The larger differences seen in Fig. 3a is attributed to the fact that

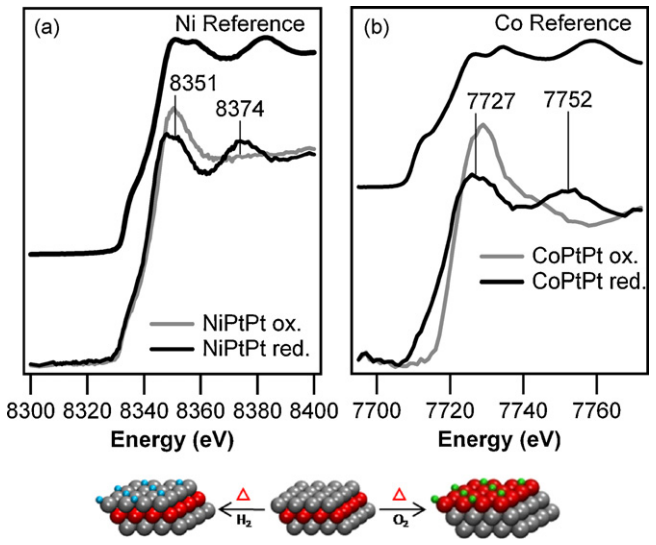

Fig. 3. (a) XANES of the Ni K-edge for a PtNiPt sample after reduction and after oxidation at room temperature and at 700 K, and (b) XANES of the Co K-edge for Co bulk reference sample, and Co–Pt–Pt sample after oxidation and reduction.

the UHV as-prepared PtNiPt sample most likely had some extent of oxygen-induced segregation since the sample was exposed to ambient atmosphere at room temperature for approximately one week during transport to the beamline. Furthermore, Fig. 3a shows that the NiPtPt and subsurface PtNiPt samples do not completely resemble the Ni reference foil (top spectrum), confirming that the Ni monolayer is not agglomerating into bulk-like particles.

As shown in Fig. 3b, CoPtPt samples exposed to H_2 and O_2 showed similar spectroscopic changes as noted for the NiPtPt system. The spectroscopic changes show similar inward diffusion of Co in H_2 and outward segregation in O_2. In addition, a higher energy Co K-edge feature is present at 7752 eV in PtCoPt and absent in CoPtPt, confirming that this higher energy feature can be potentially used as an indicator of the presence of subsurface 3d atoms in the Pt–3d–Pt structures.

In order to quantify the apparent activation barrier for the segregation of Ni at atmospheric pressure, the intensity of the white line peak at 8351 eV was monitored as a function of exposure time and temperature. The exposure series for O_2 is shown in Fig. 4 where the absorbance intensity is shown as a function of oxygen exposure in the temperature range of 633–693 K. Beginning with a subsurface

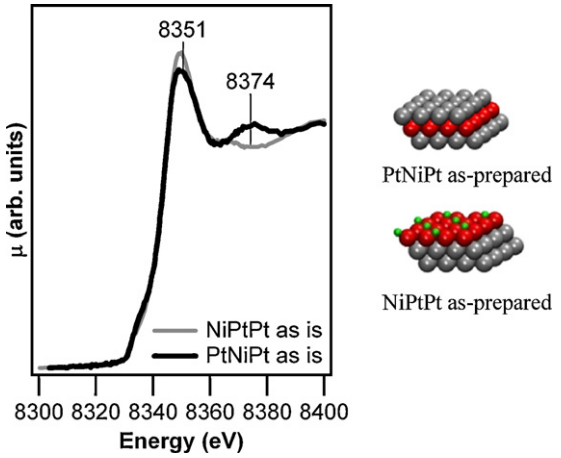

Fig. 2. XANES of the Ni K-edge for Pt–Ni–Pt and Ni–Pt–Pt as-prepared and representative structures for the as-prepared samples shown for the (1 1 1) facet.

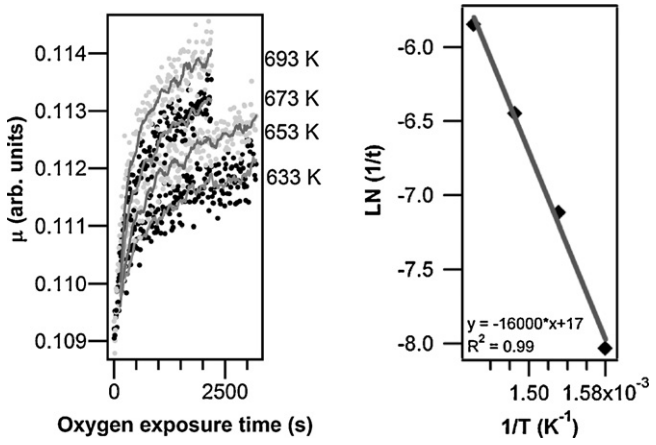

Fig. 4. (a) Intensity of Ni K edge at 8351 eV for a PtNiPt sample as a function of oxygen exposure at atmospheric pressure and (b) Arrhenius analysis for the activation barrier from PtNiPt to NiPtPt in oxygen using the time for μ to reach 0.112.

Table 1
Estimated time to achieve the segregation of approximately half of the subsurface Ni layer at different temperatures.

Temperature	Time to segregate approximately half of the subsurface Ni layer	
	From Pt(1 0 0) (current study)	From Pt(1 1 1) [17]
693 K	332 s	0.011 s
673 K	656 s	0.016 s
653 K	1352 s	0.024 s
633 K	2917 s	0.037 s
353 K (estimated)	1×10^{12} s	2200 s

configuration, as the duration to O_2 exposure increases, the white line peak absorbance increases. In addition, the disappearance of the peak at 8374 eV indicates that subsurface Ni atoms are segregating to the surface. Using an Arrhenius equation, an apparent activation barrier of 32 kcal/mol is found.

In order to correlate the rate of Ni segregation to a typical PEMFC operating temperature of 353 K, Table 1 summarizes the time it would take for the Ni K white line intensity to reach a value of $\mu = 0.112$, which corresponds to the segregation of approximately half of the subsurface Ni layer to the surface. In the second column in Table 1, the time values at 633, 653, 673 and 693 K are obtained from experiments. The time at 353 K is estimated by assuming a similar activation barrier and preexponential factor in the Arrhenius equation. As discussed in a previous study [17], the segregation of subsurface Ni atoms from polycrystalline Pt show two distinct activation barriers. The segregation from the Pt(1 0 0) region has an activation barrier similar to the one determined in the current study, while the activation barrier from the Pt(1 1 1) region has a value of 17 kcal/mol. This value is used to estimate the time for the segregation of approximately half of the subsurface Ni layer to the surface, as listed in the third column in Table 1. The values in Table 1 represent the approximate time scale for the segregation when thermal energy is provided to overcome the activation barriers. Although the values listed in Table 1 do not include the effects of applied voltage and the presence of liquid layers as in typical fuel cell operation conditions, the different trend between the segregation time from the Pt(1 0 0) and Pt(1 1 1) regions should remain the same.

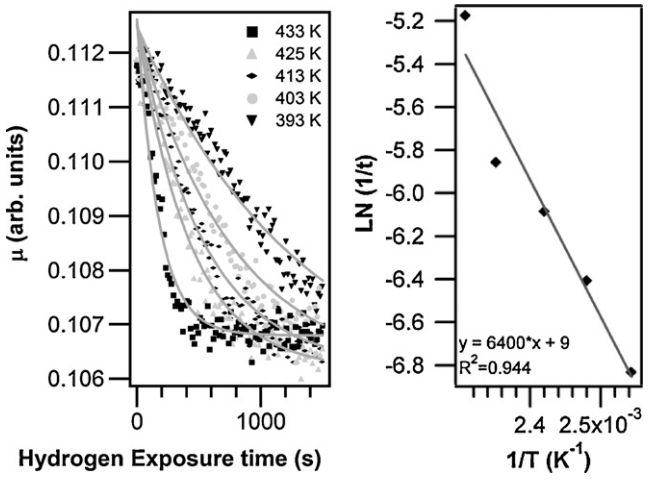

Fig. 5. (a) Intensity of Ni K edge at 8351 eV for a NiPtPt sample as a function of hydrogen exposure at atmospheric pressure and (b) Arrhenius analysis for the activation barrier from NiPtPt to PtNiPt in hydrogen using the time for μ to reach 0.109.

A similar procedure was used for monitoring the Ni reduction and diffusion into the subsurface as shown in Fig. 5. The white line peak absorbance intensity is shown to decrease with increasing exposure to hydrogen. In addition, the reappearance of the peak at 8374 eV indicates that surface Ni atoms are diffusing into the subsurface. Using the same analysis procedure, an apparent activation barrier of 13 kcal/mol is determined.

Qualitatively PtCo followed a similar diffusion and segregation process as seen for PtNi but due to the lower signal to noise ratio for the Co K edge and the lower activation barriers for PtCo, the same quantification of PtCo could not be performed at the current time. Further studies are necessary in order to optimize the experimental set-up to allow for the quantification of PtCo and other Pt–3d systems. Additional information can be obtained by employing other techniques, such as using XPS to follow the segregation of 3d metals [21] and the O K-edge regions in near-edge X-ray absorption fine structure (NEXAFS) to investigate the formation of 3d-O bonds [22].

5. Conclusions

The thermodynamically preferred configurations in O_2 and H_2 are predicted from DFT calculations and confirmed experimentally at atmospheric pressures. The subsurface Pt–3d–Pt configuration is preferred in the reducing environment of H_2 whereas the surface 3d–Pt–Pt configuration is preferred in O_2. This process has been found to be reversible, being able to cycle between the two configurations. Furthermore, the activation barrier for the segregation of subsurface Ni in atmospheric O_2 is found to be 32 kcal/mol, similar to that determined under UHV conditions. The activation barrier for hydrogen-induced diffusion of surface Ni has been determined to be approximately 13 kcal/mol. Most importantly, the in situ observation of the reversible interchange between the Pt–3d–Pt and 3d–Pt–Pt configurations at atmospheric pressure should provide useful insights into the maintenance and regeneration of the desirable subsurface structure in catalytic and electrocatalytic applications.

Acknowledgments

We acknowledge financial support from the Basic Energy Sciences of the Department of Energy (DOE/BES Grant No. DE-FG02-00ER15104).

References

[1] V. Stamenkovic, B.S. Mun, K.J.J. Mayrhofer, P.N. Ross, N.M. Markovic, J. Rossmeisl, J. Greely, J.K. Nørskov, Angewandte Chemie Interntaional Edition 45 (2006) 2897.
[2] L.E. Murillo, A.M. Goda, J.G. Chen, Journal of the American Chemical Society 129 (2007) 7101.
[3] M.P. Humbert, J.G. Chen, Journal of Catalysis 257 (2008) 297.
[4] J.G. Chen, C.A. Menning, M.A. Zellner, Surface Science Reports 63 (2008) 201.
[5] J.A. Rodriguez, Surface Science Reports 24 (1996) 225.
[6] R.A. van Santen, Theoretical Heterogeneous Catalysis, World Scientific, New Jersey, 1991.
[7] J.R. Kitchin, J.K. Norskov, M.A. Barteau, J.G. Chen, Physical Review Letters 93 (2004) 156801.
[8] C.A. Menning, H.H. Hwu, J.G. Chen, Journal of Physical Chemistry B 110 (2006) 15471.
[9] E.C. Weigert, A.L. Stottlemyer, M.B. Zellner, J.G. Chen, Journal of Physical Chemistry C 111 (2007) 14617.
[10] N.A. Khan, L.E. Murillo, J.G. Chen, Journal of Physical Chemistry B 108 (2004) 15748.
[11] J.P. Cumpson, M.P. Seah, Surface and Interface Analysis 25 (1997) 430.
[12] G. Kresse, J. Furthmuller, Computational Materials Science 6 (1996) 15.
[13] G. Kresse, J. Furthmuller, Physical Review B 54 (1996) 11169.
[14] G. Kresse, J. Hafner, Physical Review B 47 (1993) 558.

[15] *Pseudopotential Library* https://wiki.fysik.dtu.dk/dacapo/Pseudopotential_Library.
[16] C.A. Menning, J.G. Chen, Journal of Chemical Physics 130 (2009) 174709.
[17] C.A. Menning, J.G. Chen, Journal of Chemical Physics 128 (2008) 164703.
[18] D.C. Koingsberger, R. Prins (Eds.), X-ray Absorption: Principles, Applications, Techniques of EXAFS, SEXAFS, and XANES, John Wiley & Sons Inc., New York, 1988.
[19] M. Belli, A. Scafati, A. Bianconi, S. Mobilio, L. Palladino, A. Reale, E. Burattini, Solid State Communications 35 (1980) 355.
[20] H. Modrow, Applied Spectroscopy Reviews 39 (2004) 183.
[21] R.T. Mu, Q. Fu, H.Y. Liu, D.L. Tan, R.S. Zhai, X.H. Bao, Applied Surface Science 255 (2009) 7296.
[22] J.G. Chen, D.A. Fischer, J.H. Hardenbergh, R.B. Hall, Surface Science 279 (1992) 13.